Efficient phonon-assisted long-lifetime Nd^{3+} fluorescence in $Cs_2NaNdCl_6$

B. C. Tofield* and H. P. Weber
Bell Laboratories, Holmdel, New Jersey 07733
(Received 9 July 1974)

Spectroscopic measurements are reported on single crystals of the high-Nd^{3+}-concentration perovskite $Cs_2NaNdCl_6$ [$\rho(Nd) = 3.2 \times 10^{21}$ cm^{-3}] and on $Cs_2NaNd_{0.01}Y_{0.99}Cl_6$. The room-temperature fluorescence lifetimes are 1.23 and 4.1 msec, respectively, which are the longest reported so far for Nd^{3+} in any environment. This compound shows weak concentration quenching of fluorescence comparable to that observed in NdP_5O_{14} which has $\rho(Nd) = 4 \times 10^{21}$ cm^{-3}. This is related to the isolation of the Nd^{3+} ions which are located in discrete $NdCl_6^{3-}$ octahedra and have a minimum separation of 0.77 nm. The long fluorescence lifetime results from the strict octahedral coordination of Nd^{3+} which discourages electric-dipole electronic transitions. Absorption and emission of the $^4F_{3/2} - {}^4I_{9/2}$ and $^4F_{3/2} - {}^4I_{11/2}$ levels are found to be dominated by phonon-assisted vibronic transitions. The ground state to the $^4F_{3/2}$ no-phonon line is observed in absorption at 1.8 °K, and the phonon-assisted spectra at shorter wavelengths are used to interpret the $^4F_{3/2}$ to $^4I_{9/2}$ emission spectra at 1.8 °K. The phonon-assisted spectra associated with the $^4F_{3/2}$ to $^4I_{11/2}$ emission are not the same as observed for the $^4F_{3/2}$ to $^4I_{9/2}$ emission but a tentative assignment has been made. Due to the reduction of the phonon populations at lower temperatures the emission cross sections are reduced and the lifetimes of the concentrated and dilute crystals increase to 5 and 11 msec, respectively, at 77 °K. A comparison with YAG : Nd and NdP_5O_{14} indicates that ~ 5% of absorbed photons are emitted into the $^4I_{11/2}$ levels in $Cs_2NaNdCl_6$ at room temperature, and an approximate peak emission cross section of 1.2×10^{-21} cm^2 is calculated for the $^4F_{3/2}$ to $^4I_{11/2}$ emission. This is ~ 100 times lower than found for NdP_5O_{14} and indicates a low gain in pulsed laser operation. Because of the far longer lifetime, however, the gain per ion under cw operation is predicted to be ~ 10 times lower than for NdP_5O_{14} and ~ 7 times lower if diluted samples of the two compounds are compared with each other.

INTRODUCTION

The study of the fluorescence properties of rare-earth ions in crystals provides both an insight into fundamental interactions in solids[1] and is also of considerable practical interest. In particular, the use of fluorescing materials for laser applications[2] and for fluorescing up-converters[3] are intensively studied applications. Almost all such studies have been carried out on systems where the rare earth is in a local environment lacking a center of symmetry.[4] In such cases the forbiddenness of the f-f electric-dipole transitions is lifted somewhat by interactions with odd-parity states via the crystal field. These transitions are thus partially allowed and are often observed to be accompanied by considerably weaker phonon-assisted (vibronic) transitions [e.g., for Pr^{3+} in LaF_3,[5] Pr^{3+} and Nd^{3+} in $NdCl_3$,[6] and Ho^{3+} in BaY_2F_8 (Ref. 7)].

On the other hand if the rare-earth ion is situated at a center of symmetry, pure electric-dipole transitions are strongly forbidden. Only infrared phonon-assisted electric-dipole transitions and weakly allowed magnetic-dipole transitions will be observed. Moreover, it has been suggested[8] that excited states of rare-earth ions in such an environment might have very long relaxation times. This offers interesting possibilities for laser action and energy storage and transfer.

We report in this study some spectroscopic properties of Nd^{3+} in the perovskite $Cs_2NaNdCl_6$. The Na^+ and Nd^{3+} ions are ordered on the octahedral sites so that the lattice parameter (1.0889 nm) is double that of the simple perovskite cell (Fig. 1) and both ions are on sites of point symmetry $m3m$. The closest Nd^{3+}-Nd^{3+} distance is 0.77 nm and no anions are nearest neighbors to more than one Nd^{3+}, these ions being separated by a Cl-Na-Cl chain. The Nd^{3+} ions are arranged on a face-centered-cubic sublattice and thus the Nd^{3+} concentration (3.2×10^{21} per cm^3) is the maximum possible for the given separation.

In spite of the large Nd^{3+}-Nd^{3+} separation, the concentration of neodymium ions is over twenty times greater than that which can be used in conventional laser hosts such as YAG : Nd. At higher Nd^{3+} concentrations in YAG, fluorescence quenching of the 1.06-μm $^4F_{3/2} - {}^4I_{11/2}$ emission arising via nonradiative decay from Nd-pair interactions is observed. In YAG, however, the nearest-neighbor rare-earth–rare-earth separation may be as low as 0.37 nm, and recent studies on the high-Nd^{3+}-concentration material neodymium pentaphosphate (NdP_5O_{14}),[9] where the nearest Nd^{3+}-Nd^{3+} distance is 0.519 nm, have shown that fluorescence quenching is not severe, despite the high Nd^{3+} concentration (~ 4×10^{21} per cm^3). It is thought that this is caused by the large rare-earth separation and by the position of the $^4I_{15/2}$ level be-

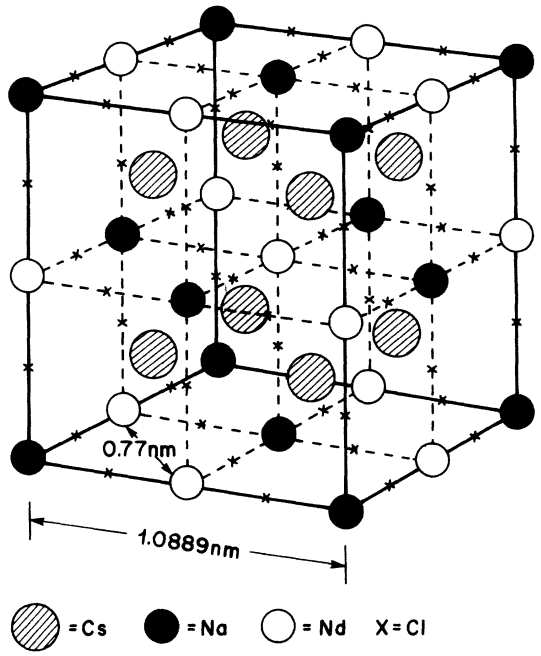

FIG. 1. Crystal structure of $Cs_2NaNdCl_6$.

ing unfavorable for inducing nonradiative decay by pair interaction.

In $Cs_2NaNdCl_6$ the Nd^{3+} concentration is only 20% less than in NdP_5O_{14}, but the minimum separation is 50% greater. As well as allowing the study of rare-earth absorption and fluorescence spectra and excited-state lifetimes in an octahedral crystal field, this host also allows a further investigation of the effect of the Nd^{3+}-Nd^{3+} separation on the fluorescence quenching of the $^4F_{3/2} \rightarrow {}^4I_{11/2}$ transition. If one assumes an electric-dipole interaction for this process, with an r^{-6} dependence on distance, the crucial role of the rare-earth separation distance becomes apparent.

We have studied the infrared emission from the $^4F_{3/2}$ to the $^4I_{11/2}$ and $^4I_{9/2}$ levels and absorption from $^4I_{9/2}$ to $^4F_{3/2}$ at 300, 77, and 1.8 °K. The crystal-field levels of the $^4I_{9/2}$ and $^4I_{11/2}$ manifolds have been tentatively assigned, and the $^4F_{3/2}$ lifetime has been measured at 300 °K and at 77 °K in $Cs_2NaNdCl_6$ and $Cs_2NaNd_{0.01}Y_{0.99}Cl_6$. Although we have chosen to study Nd^{3+} because of the associated interest in Nd^{3+}-Nd^{3+} interactions, the chloride host will accept all the rare-earth ions (and several other trivalent metal ions) and studies on other ions will be interesting. Apart from measurements on rare-earth ions doped into cubic crystals such as CaF_2 and CaO where the necessity to charge compensate generally produces several sites of different symmetry with associated problems of interpretation, we are aware of no previous detailed optical studies of f-f transitions for trivalent rare earths in octahedral sites in crystals. In the same host the magnetic susceptibility of Yb^{3+} has been reported[10] with as assignment of the ground-state crystal-field splitting, and the electric-dipole allowed $4f^1 \rightarrow 5d^1$ transition of Ce^{3+} has been studied by absorption and magnetic-circular-dichroism spectra.[11]

CRYSTAL GROWTH

Crystals of $Cs_2NaNdCl_6$ and $Cs_2NaNd_{1-x}Y_xCl_6$ ($x \approx 0.99$) were grown by the Bridgman method in evacuated quartz ampoules at 800–850 °C. Starting materials were anhydrous 99.999% $NdCl_3$ and YCl_3 (Research Chemicals), 99.99% CsCl (Gallard-Schlesinger) and "AnalaR" NaCl (British Drug Houses). The alkali halides were dried under vacuum at 500–600 °C before use and the rare-earth chlorides purified by vacuum sublimation. All subsequent handling and mixing was performed in a nitrogen-filled dry box.

Debye-Scherrer x-ray photographs of the powdered crystals showed the expected superlattice lines indicating Na-Nd ordering, and the high-angle lines showed no splittings which would be indicative of distortions from cubic symmetry. No impurity lines were observed and the lattice parameters agreed with those given by Morss *et al.*[12]

Pure polycrystalline samples were also prepared by evaporation to dryness of solutions of the mixed chlorides in concentrated hydrochloric acid. The fluorescence lifetimes observed for these samples were in agreement with those obtained for the single crystals, indicating freedom from hy-

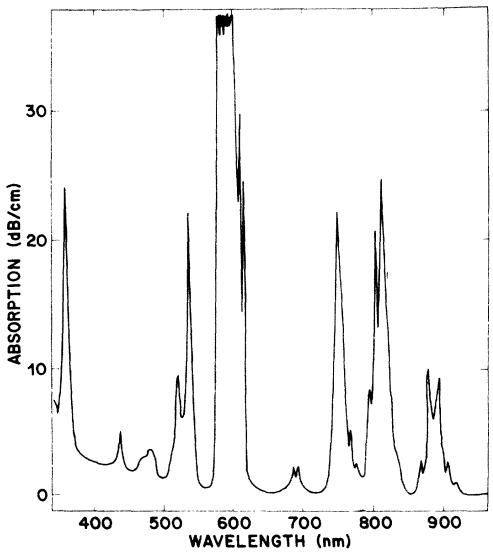

FIG. 2. Absorption spectrum of $Cs_2NaNdCl_6$ at 300 °K. Sample thickness 5 mm.

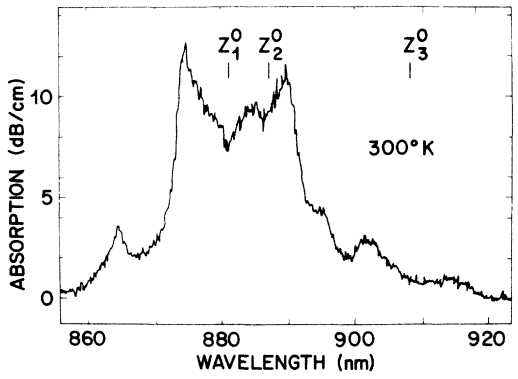

FIG. 3. Absorption spectrum of $Cs_2NaNdCl_6$ around 880 nm at 300°K. Sample thickness 5 mm. The positions of the no-phonon $^4F_{3/2} - {}^4I_{9/2}$ lines Z_1^0, Z_2^0, and Z_3^0 are indicated.

drogen-containing impurities.

The perovskite chlorides are considerably more stable to attack by atmospheric moisture than the rare-earth trichlorides, and the measurements reported here could be carried out without special sample-handling procedures.

SPECTROSCOPY

Absorption

The crystal was cut into a platelet of 5 mm thickness and polished on a dry lap with Linde 1-μm alumina abrasive powder. The room-temperature absorption spectrum, measured with a model 14R Cary recording spectrometer, is shown in Fig. 2. The strengths of the absorption bands at 750 and 800 nm are about 30 times weaker than in NdP_5O_{14} while the absorption bands in the visible range are about 10 times weaker. The widths of the lines are comparable to those found in NdP_5O_{14}.[13]

The absorption around 880 nm is shown in more detail in Fig. 3. This is the transition from the ground-state manifold ($^4I_{9/2}$) to the $^4F_{3/2}$ manifold. The energy-level diagram of Nd^{3+} in an octahedral crystal field is simpler than in lower-symmetry environments. In particular the $^4F_{3/2}$ level is unsplit and the $^4I_{9/2}$ ground-state and $^4I_{11/2}$ lower laser-state manifolds split into three and four levels, respectively, as shown in Fig. 4. The $^4I_{13/2}$ and $^4I_{15/2}$ manifolds both split into five levels. The room-temperature absorption spectrum is dominated by phonon-assisted transitions, however, and no estimate of the ground-state splittings can be made. The no-phonon lines determined from the liquid-helium spectra are indicated (we use the conventional nomenclature to describe the Nd^{3+} infrared lines).

More information can be gained from absorption measurements at 1.8°K. Only the lowest ground-

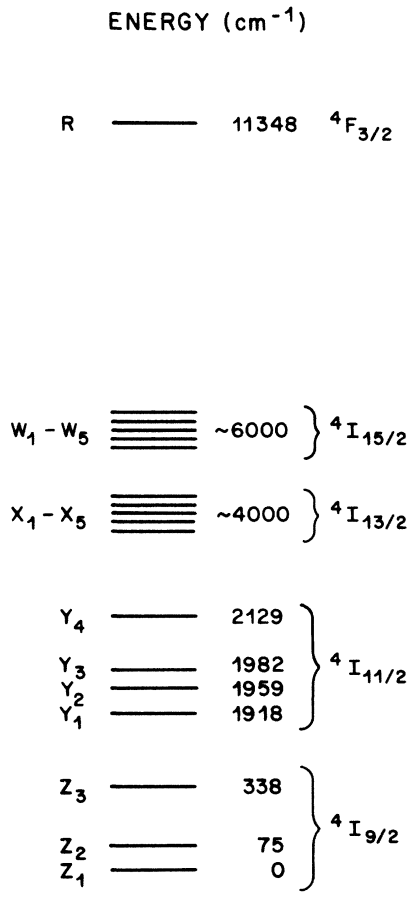

FIG. 4. Partial energy-level diagram of Nd^{3+} in $Cs_2NaNdCl_6$ (not to scale).

state level will be occupied so that a single electronic $^4I_{9/2} - {}^4F_{3/2}$ transition should be seen. The measured spectrum is shown in Fig. 5. The transmission of light from an incandescent filament was measured with a 1-m grating spectrometer and a cooled photomultiplier with an S1 cathode. The light was modulated with a chopper and a lock-in amplifier was used. A single sharp line is ob-

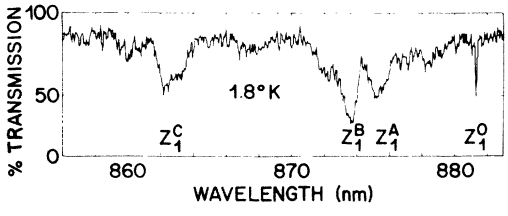

FIG. 5. Transmission spectrum of $Cs_2NaNdCl_6$ around 880 nm at 1.8°K. Sample thickness 5 mm, resolution 0.05 nm. The no-phonon line Z_1^0 and the regions of maximum phonon-assisted intensity Z_1^A, Z_1^B, and Z_1^C are indicated.

served at 881.2 nm. Its width of 0.05 nm corresponds to the resolution limit of the apparatus. Broad absorption bands of significantly greater intensity are observed at higher energy and extend to $\approx$ 860 nm. We interpret the 881.2-nm line as the no-phonon magnetic-dipole $^4I_{9/2}$ ground state to $^4F_{3/2}$ transition, and this is confirmed by the 1.8 °K emission spectrum (see below). The broad lines are interpreted as phonon-assisted electric-dipole transitions. At 1.8 °K the photon absorption is associated with the emission of a phonon so that these transitions show a blue shift relative to the electronic transition frequency. The phonon-assisted bands extend to ≈ 280 cm^{-1} from the no-phonon line. This agrees with the energies of the vibronic side bands observed for Ce^{3+} in Cs_2NaYCl_6,[11] and is consistent with an expected phonon cutoff frequency of ≈ 300 cm^{-1} for this structure.

According to Yen *et al.*[5] the intensity distribution $I(\omega)$ of the phonon side bands at zero temperature is simply related to the phonon density of states $\rho(\omega)$,

$$\rho(\omega) \propto I(\omega)\omega, \tag{1}$$

and they showed the effective $\rho(\omega)$ versus phonon frequency for the Pr^{3+} $^3H_4 \rightarrow {}^3P_0$ absorption observed in LaF_3. However, as was pointed out by Cohen and Moos,[6] the relative intensities of the vibronic transitions do not necessarily indicate the actual relative strength of the peaks of $\rho(\omega)$ since the coupling coefficients between the electronic excitation and the infrared phonons need not be constant and therefore we have not converted the intensities of Fig. 5 according to Eq. (1).

The intensity distribution of the vibronic transitions is relatively simple, although the phonon spectrum should have 120 branches, and we have labeled the dominant features Z_1^A, Z_1^B, and Z_1^C (the no-phonon line is labeled Z_1^0). It is likely that these reflect a high density of infrared phonon states and/or large dipole moments at these energies (~ 80, ~ 100, and 240–250 cm^{-1}, respectively). If, as found for Pr^{3+} and Nd^{3+} in $NdCl_3$,[6] these vibronic lines are due to flat portions of phonon branches with wave vectors above directions of high symmetry in the Brillouin zone it should be possible to relate them to $\vec{k} = 0$ modes in the infrared spectrum.

As already discussed, vibronic transitions have been previously studied for Pr^{3+}, Nd^{3+}, and other rare-earth ions, and phonon-terminated laser action has recently been observed at 2.17 μm for line $^5I_7$ to $^5I_8$ of Ho^{3+} in BaY_2F_8.[7] However, because of the high Nd^{3+} site symmetry which forbids no-phonon electric-dipole transitions, the phonon-assisted transitions observed in this work are unique for trivalent rare-earth ions insofar as their strengths are far greater than those of the no-phonon lines.

Emission

The fluorescence at 1.8 °K from the same sample was measured in transmission with excitation by the 514.5-nm line of an Ar-ion laser. The pump beam passed first through a Schott BG 18 infrared absorption filter, was modulated with a chopper wheel, and was focused onto the sample. The fluorescence was collected with a lens and focused onto the slit of a 1-m grating spectrometer, and a lock-in amplifier was again used.

The emission into the $^4I_{9/2}$ ground-state manifold is shown in Fig. 6. The spectrum is reproducible from run to run. Because we are now observing transitions to three $^4I_{9/2}$ levels, the assignment is not so straightforward as with the ground-state absorption. However, we anticipate similar phonon-assisted spectra as observed in absorption, since the same electronic levels are involved, except that in emission these will be red shifted relative to the no-phonon energy, the photon emission being associated with phonon emission. The highest-energy line at 881.2 nm corresponds with the no-phonon line observed in absorption. By matching the phonon-assisted spectra to those found in absorption we assign the other two no-phonon magnetic-dipole transitions at 887.1 and 908.3 nm. These are indicated on Fig. 6. Each line is associated with strong phonon-assisted transitions at ~ 80–120 and ~ 240–250 cm^{-1} as well as weaker bands at ~ 40 and ~ 270–280 cm^{-1} also seen in absorption. A qualitative assignment of the phonon-assisted intensities A, B, and C (Fig. 5) between the three bands is also shown in Fig. 6.

The emission spectra at 77 and 300 °K are given in Fig. 7, and these spectra also are reproducible from run to run. The positions of the no-phonon lines deduced from Fig. 6 are indicated. The appearance of blue-shifted phonon-absorption-assisted lines at the higher temperatures makes the analysis of these spectra impossible without the evidence gained from the low-temperature spectra.

Fluorescence into the $^4I_{11/2}$ manifold is shown in Fig. 8 (1.8 °K) and Fig. 9 (77 and 300 °K), together with the assignments. Once again the high-temperature spectra show considerable structure associated with phonon absorption. A consistent assignment of the spectrum at 1.8 °K cannot be made by assuming similar phonon-assisted spectra as for the $^4F_{3/2} \rightarrow {}^4I_{9/2}$ transitions, and the appearance of several sharp lines in the emission precludes the assignment of the magnetic-dipole transitions on this basis. Our assignment is based on the observation of four broad phonon-assisted peaks at ~ 1090, ~ 1094, ~ 1097 (Fig. 8) and ~ 1114

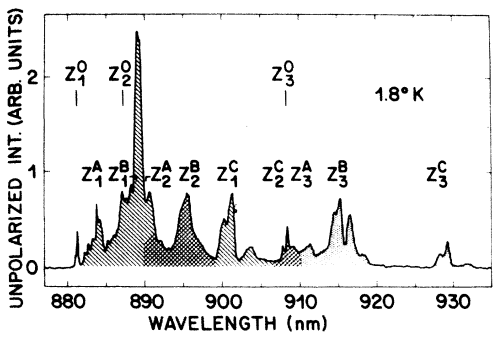

FIG. 6. Emission spectrum of $Cs_2NaNdCl_6$ around 900 nm at 1.8°K. Sample thickness 5 mm, resolution 0.14 nm. The positions of the three no-phonon lines Z_1^0, Z_2^0, and Z_3^0 and the regions of maximum phonon-assisted intensity associated with these are labeled and also indicated by shading.

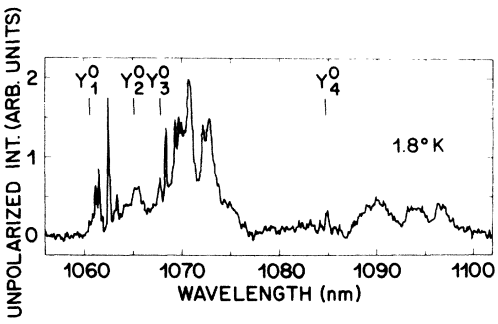

FIG. 8. Emission spectrum of $Cs_2NaNdCl_6$ around 1070 nm at 1.8°K. Sample thickness 5 mm, resolution 0.14 nm. The positions of the four no-phonon $^4F_{3/2} - {}^4I_{11/2}$ lines, Y_1^0, Y_2^0, Y_3^0, and Y_4^0 are indicated.

nm (Fig. 9). The first of these is ~250 cm^{-1} from the high-energy end of the spectrum and the latter a similar energy below the feature at 1085 nm. It seems reasonable that all four represent phonon-assisted transitions at ~250 cm^{-1} from no-phonon lines, and on this basis the no-phonon magnetic-dipole lines are assigned to features at 1060.5, 1065.1, 1067.7, and 1084.7 nm. The vibronic spectra are different from the $^4I_{9/2}$ vibronic spectra, showing intensity with several sharp lines up to ~40 cm^{-1} and then little intensity before the broad bands at ~250 cm^{-1}, which is a feature in common with the $^4I_{9/2}$ spectra.

The emission spectra at 77 and 300°K are corrected for the spectral sensitivity of the detection system; in the 1.8°K spectra this correction has not been made. All the 77 and 300°K emission spectra were measured on samples ~0.3 mm thick, which guarantees a negligible modification of the intensity due to reabsorption.

The tentative energy-level diagram showing the level positions determined for the $^4I_{9/2}$, $^4I_{11/2}$, and $^4F_{3/2}$ bands is given in Fig. 4. The expected positions of the $^4I_{15/2}$ and $^4I_{13/2}$ levels are also shown.

In the work reported here, we have not been primarily concerned with the interpretation of the observed crystal-field splittings. However, we should note that an octahedral environment provides a relatively simple situation to study crystal-field effects for rare-earth ions since the splittings

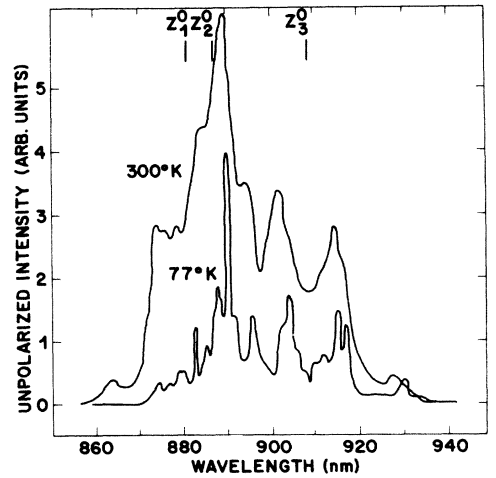

FIG. 7. Emission spectra of $Cs_2NaNdCl_6$ around 900 nm at 77 and 300°K measured with a 0.3-mm thick sample. Spectral resolution 0.5 nm. These spectra are corrected for the spectral sensitivity variation of the detection system. The positions of the three no-phonon lines Z_1^0, Z_2^0, and Z_3^0 are indicated.

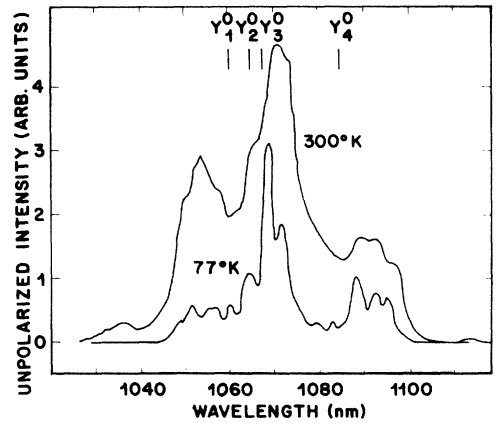

FIG. 9. Emission spectra of $Cs_2NaNdCl_6$ around 1070 nm at 77 and 300°K measured with a 0.3-mm-thick sample. Spectral resolution 0.5 nm. These spectra are corrected for the spectral sensitivity variation of the detection system. The intensity scale has the same units as Fig. 7. The positions of the four no-phonon lines Y_1^0, Y_2^0, Y_3^0, and Y_4^0 are indicated.

can be defined by only two parameters, b_4 and b_6.[14] A value for the ratio b_4/b_6 between -100 and -270 was shown to be consistent with the magnetic susceptibility of Yb^{3+} in $Cs_2NaYbCl_6$,[10] and an approximate conversion to the value expected for Nd^{3+} using the parameters listed by Ref. 14 indicates that b_4/b_6 is $\gg 1$, which would imply a Γ_8^1 ground state with the first excited state being Γ_6 and the second Γ_8^2. This assignment can be checked by electron-spin resonance on a dilute sample. This host is clearly attractive in studying the crystal-field parameters of all the rare-earth ions in a strictly octahedral environment when the no-phonon lines can be identified.

Nd^{3+} FLUORESCENCE LIFETIME

The fluorescence lifetime of the $^4F_{3/2}$ level was measured by exciting the crystal with a pulsed flashlamp pumped Rhodamine 6G dye laser, tuned to the 590-nm absorption band. In accordance with the highly forbidden nature of the electronic transitions observed, very long fluorescence lifetimes are expected. At room temperature the lifetime of $Cs_2NaNdCl_6$ was 1.23 msec. The highest lifetimes previously observed (in dilute systems) at room temperature were 0.9 msec in K-Rb-Ba-Si glass,[15] 1.5 msec in CaF_2,[16] and 0.7 msec in $BaGd_{0.48}Nd_{0.02}Ta_{0.05}O_3$.[17] This latter crystal is the oxide analog of the chlorides studied in this work.

In order to investigate the degree of concentration quenching, a crystal of composition $Cs_2NaNd_{0.01}Y_{0.99}Cl_6$ was also grown. The room-temperature lifetime was 4.1 msec. It seems unlikely that the emission cross section is changing with Nd^{3+} concentration. The symmetry is unchanged and the room-temperature absorption and emission spectra are qualitatively very similar for the dilute and concentrated samples. It appears, therefore, that concentration quenching still exists, even at 0.77-nm Nd-Nd separation; it is small and similar to that observed in NdP_5O_{14}. Although we have not determined the position of the intermediate $^4I_{15/2}$ level which can provide an efficient quenching mechanism[18] it nevertheless seems that an adequate interpretation of the variation of fluorescence quenching from one material to another, taking into account both intermediate-level positions and the minimum Nd-Nd separation, has still to be given. This evidence for interactions between the ions, together with the long fluorescent lifetimes, does however, make this host an attractive candidate for energy-transfer studies and application.

In the case of dominant phonon-assisted transitions one expects the lifetime to be temperature dependent, as has been reported for the phonon-induced transitions in Pr^{3+}.[5] At low temperature, only assistance due to spontaneous phonon emission can take place. At higher temperature stimulated phonon emission and also phonon absorption can assist the photon emission. Consequently the emission cross sections become larger and the lifetimes shorten. At 77 °K we observe lifetimes of 5 msec for $Cs_2NaNdCl_6$ and 11 msec for the diluted crystal, in qualitative agreement with this expectation.

EMISSION CROSS SECTIONS

A measurement of the phonon-assisted emission cross sections is rather difficult to perform. The usual method for such measurements is based on the assumption of the equality of absorption and emission cross sections. This can only be applied to the no-phonon lines, however, because the phonon-assisted lines in absorption and emission are not identical (photon absorption plus phonon emission versus photon emission plus phonon emission). A calibration of the no-phonon lines was not possible because the lines are narrower than the resolution limit (~0.20 nm) of our detection system and also because many of these lines overlap significantly with phonon-assisted intensity.

By integrating the intensities in Figs. 7 and 9, however, one evaluates a branching ratio of 1 : 1 for the transitions into the $^4I_{9/2}$ and $^4I_{11/2}$ bands at 300 °K. In order to learn about the fluorescence efficiency we made a relative measurement at room temperature using samples of YAG : Nd, NdP_5O_{14} (samples with $\tau_f = 66$ μsec),[9] and $Cs_2NaNdCl_6$. The samples were excited with the 520.8-nm beam of a Kr-ion laser, and the fluorescence into the $^4I_{9/2}$ band was monitored using broadband optical filters and a cooled photomultiplier with an S1 cathode. The same geometry was used for all three measurements. The relative fluorescence yields were 1 : 1.18 : 0.16. The fluorescent yields into the $^4I_{9/2}$ band have been reported to be about 32% for both YAG : Nd (Ref. 19), and $Nd_xLa_{1-x}P_5O_{14}$ (Ref. 20) in the zero-concentration limit with $\tau_f = 300$ μsec. Using our measured values for YAG : Nd and NdP_5O_{14} as calibration, we find the fluorescent yield for $Cs_2NaNdCl_6$ into this band to be approximately 5%.

The increase of the $^4F_{3/2}$ lifetime from 1.23 msec for the concentrated crystal to 4.1 msec for the diluted crystal implies an increase in fluorescence efficiency into the $^4I_{9/2}$ band to approximately 17%, and the integrated intensities indicate a similar yield into $^4I_{11/2}$. This is somewhat lower than in YAG and NdP_5O_{14}, where the fluorescent yield into this level is about 60%. The experimental measurement probably gives a lower limit for the fluorescent yield, however, and the absorbed energy unaccounted for by fluorescence into $^4I_{9/2}$ and

$^4I_{11/2}$ may be less than 66% indicated by this measurement. Multiphonon non-radiative decay is unlikely since the $^4F_{3/2}$ to $^4I_{15/2}$ transition would require at least 17 phonons if a phonon cutoff of 300 cm^{-1} is assumed. Fluorescence into $^4I_{15/2}$ and $^4I_{13/2}$ is weak in other compounds but may be relatively stronger in this case because of the dominance of phonon-assisted transitions.

We may make a rough estimate of the peak emission cross section in $Cs_2NaNdCl_6$ at room temperature by comparing the fluorescence efficiency, the emission linewidths of the $^4F_{3/2} - {}^4I_{11/2}$ transitions, and the lifetimes of diluted samples of NdP_5O_{14} and $Cs_2NaNdCl_6$. We use the relation

$$\sigma_{C1} = \sigma_{PP} \frac{\eta_{C1}\tau_{PP}\Delta\lambda_{PP}}{\eta_{PP}\tau_{C1}\Delta\lambda_{C1}} , \qquad (2)$$

where τ is the fluorescence lifetime, σ is the emission cross section, η the fluorescence efficiency, $\Delta\lambda$ the linewidth of a particular transition, and the subscripts C1 and PP refer to the hexachloride and pentaphosphate, respectively. The peak effective emission cross section in NdP_5O_{14} is 1.2×10^{19} cm^2,[20] $\tau_{PP} = 300$ μsec, $\tau_{C1} = 4100$ μsec, $\Delta\lambda_{PP}/\Delta\lambda_{C1} \sim 0.5$, $\eta_{PP} \sim 0.6$, and $\eta_{C1} \sim 0.17$, giving $\sigma_{C1} \sim 1.2\times10^{-21}$ cm^2, which is 100 times smaller than found for NdP_5O_{14}.

CONCLUSIONS

We have investigated a new high-concentration Nd compound, $Cs_2NaNdCl_6$, in which concentration quenching of fluorescence is small. The crystal symmetry forbids direct electric-dipole transitions, and fluorescence takes place almost exclusively via phonon-assisted decay. From absorption and emission spectra at 1.8 °K, the no-phonon magnetic-dipole electronic lines for the $^4F_{3/2} - {}^4I_{9/2}$ and $^4F_{3/2} - {}^4I_{11/2}$ transitions have been tentatively assigned. The dominant vibronic transitions extend for ≈ 280 cm^{-1} providing a qualitative estimate of the phonon cutoff.

The room-temperature fluorescence lifetimes of 1.23 msec for the concentrated and 4.1 msec for diluted crystals are the longest so far found for Nd in any material. The total fluorescence efficiency from $^4F_{3/2}$ into $^4I_{9/2}$ and $^4I_{11/2}$ is about 34% in dilute $Cs_2NaY_{1-x}Nd_xCl_6$.

The peak emission cross section for the $^4F_{3/2}$ to $^4I_{11/2}$ transition has been estimated to be $\sigma \sim 1.2\times10^{-21}$ cm^2 at room temperature, about 100 times lower than in NdP_5O_{14}. This means that the net gain per pumped ion in stimulated emission will also be 100 times lower than in NdPP for pulsed excitation. Conversely the energy storage capability for a laser of this material is ~ 100 times higher. Due to the long fluorescence lifetime, however, the optical gain per pumped ion that one expects under cw pumping is only about 10 times lower than in NdP_5O_{14} and seven times lower if one compares the two diluted materials. The observed interaction between Nd ions and the long lifetime may lead to efficient energy diffusion which could facilitate single-frequency cw operation.[21] Such a laser should also be tunable over the whole bandwidth from 1.05 to 1.10 μm. This material is also attractive in that it can readily be grown with any other rare-earth ion or with any combination of them and also with the rare earth substituted by transition-metal ions, which offers the possibility of constructing efficient upconverters and sensitized laser materials.

The bromide analogs of the materials reported here have not been reported although we imagine they should exist. Although isostructural fluorides containing neodymium have not been reported[22,23] it seems likely that they will exist with the correct combination of atoms, and all the heavier rare earths (M) other than Nd occur in the cubic compounds Rb_2NaMF_6 and Cs_2NaMF_6.[22] The spectroscopic properties both of such fluorides and bromides and of the isostructural oxides such as Ba_2NbNdO_6 (Ref. 17) are expected to be similar to those reported here, although differences in phonon energies and crystal-field and bonding parameters may also bring about interesting differences.

ACKNOWLEDGMENTS

We would like to thank L. F. Mollenauer for making his equipment available for the 1.8 °K investigations. We thank also A. Kiel and J. M. Worlock for several helpful discussions concerning the interpretation of the spectra.

*Present address: Materials Physics Division, A.E.R.E., Harwell, Oxfordshire, England.

[1]See, e.g., B. DiBartolo, *Optical Interactions in Solids* (Wiley, New York, 1968).

[2]See, e.g., M. J. Weber, in *Handbook of Lasers* (Chemical Rubber Co., Cleveland, 1971), pp. 371–417.

[3]See, e.g., L. F. Johnson, H. J. Guggenheim, T. C. Rich, and F. W. Ostermayer, J. Appl. Phys. 43, 1125 (1972).

[4]For example, in the case of YAG:Nd and NdP_5O_{14} the Nd^{3+} point symmetry is 222 and 1, respectively.

[5]W. M. Yen, D. C. Scott and A. L. Schawlow, Phys. Rev. 136, A271 (1964).

[6]E. Cohen and H. W. Moos, Phys. Rev. 161, 258 (1967); 161, 268 (1967).

[7]L. F. Johnson and H. J. Guggenheim, IEEE J. Quantum Electron. QE-10, 442 (1974).

[8]G. H. Dieke, *Spectra and Energy Levels of Rare Earth Ions in Crystals* (Interscience, New York, 1968).

[9]B. C. Tofield, H. P. Weber, T. C. Damen, and G. A.

Pasteur, Mater. Res. Bull. 9, 435 (1974); and B. C. Tofield, H. P. Weber, T. C. Damen, and P. F. Liao, J. Solid State Chem. (to be published).
[10]D. G. Karraker, J. Chem. Phys. 55, 1084 (1971).
[11]R. W. Schwartz and P. N. Schatz, Phys. Rev. B 8, 3229 (1973).
[12]R. L. Morss, M. Siegal, L. Stenger, and N. Edelstein, Inorg. Chem. 9, 1771 (1970).
[13]H. G. Danielmeyer and H. P. Weber, IEEE J. Quantum Electron. QE-8, 805 (1972); M. Blätte, H. G. Danielmeyer, and R. Ulrich, Appl. Phys. 1, 275 (1973).
[14]K. R. Lea, M. J. M. Leask, and W. P. Wolf, J. Phys. Chem. Solids 23, 138 (1962).
[15]E. Snitzer, Appl. Opt. 5, 1487 (1966).
[16]A. A. Kaminskii, L. S. Kornienko, and A. M. Prokhorov, Zh. Eksp. Teor. Fiz. 48, 476 (1965) [Sov. Phys.-JETP 21, 318 (1965)].
[17]F. S. Galasso, G. K. Layden, and D. E. Flinchbaugh, J. Chem. Phys. 44, 2703 (1966).
[18]G. E. Peterson and P. M. Bridenbaugh, J. Opt. Soc. Am. 54, 644 (1964).
[19]S. Singh, R. G. Smith and L. G. Van Uitert, Phys. Rev. B 10, 2566 (1974).
[20]H. P. Weber, P. F. Liao, and B. C. Tofield, IEEE J. Quantum Electron. QE-10, 563 (1974).
[21]H. P. Weber, B. C. Tofield, and T. C. Damen, Paper MB8, Digest of Technical Papers, Topical Meeting on Integrated Optics, New Oreans, 1974 (unpublished).
[22]S. Aléonard and C. Pouzet, J. Appl. Crystallogr. 1, 113 (1968).
[23]J. B. Goodenough and J. M. Longo, in *Landolt-Börnstein, Numerical Data and Functional Data in Science and Technology, New Series*, edited by K. H. Hellwege (Springer, New York, 1970), Group III, Vol. 4a, p. 131.

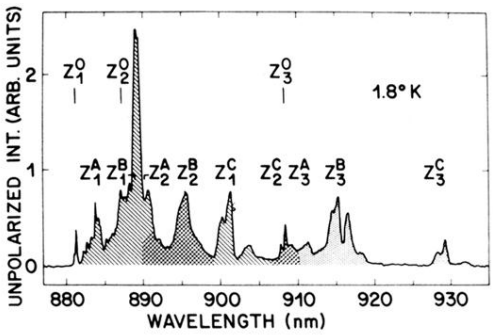

FIG. 6. Emission spectrum of $Cs_2NaNdCl_6$ around 900 nm at 1.8°K. Sample thickness 5 mm, resolution 0.14 nm. The positions of the three no-phonon lines Z_1^0, Z_2^0, and Z_3^0 and the regions of maximum phonon-assisted intensity associated with these are labeled and also indicated by shading.